Colloidal Spheres

International Edition: DOI: 10.1002/anie.201805781
German Edition: DOI: 10.1002/ange.201805781

Sol–Gel Synthesis of Metal–Phenolic Coordination Spheres and Their Derived Carbon Composites

Jing Wei[+], *Gen Wang*[+], *Feng Chen*[+], *Min Bai, Yan Liang, Huanting Wang, Dongyuan Zhao, and Yongxi Zhao**

Abstract: *A formaldehyde-assisted metal–ligand crosslinking strategy is used for the synthesis of metal–phenolic coordination spheres based on sol–gel chemistry. A range of mono-metal (Co, Fe, Al, Ni, Cu, Zn, Ce), bi-metal (Fe-Co, Co-Zn) and multi-metal (Fe-Co-Ni-Cu-Zn) species can be incorporated into the frameworks of the colloidal spheres. The formation of coordination spheres involves the pre-crosslinking of plant polyphenol (such as tannic acid) by formaldehyde in alkaline ethanol/water solvents, followed by the aggregation assembly of polyphenol oligomers via metal–ligand crosslinking. The coordination spheres can be used as sensors for the analysis of nucleic acid variants with single-nucleotide discrimination, and a versatile precursor for electrode materials with high electrocatalytic performance.*

Colloidal spheres have been widely applied in optics, biomedicine, biosensor, catalysis, and energy.[1] Various methods, such as sol–gel process and hydrothermal synthesis, have been developed to prepare colloidal spheres. As a typical case, the Stöber method has been widely used to synthesize colloidal silica spheres in the alkaline alcohol/water solvents.[2] Based on the sol–gel synthesis, a variety of inorganic and polymeric spheres (such as resorcinol-formaldehyde resin spheres) were obtained.[3] Most importantly, combining with other techniques (for example, spin coating), various functional composites could be fabricated, which would greatly extend the applications of colloidal spheres.[4] Metal–organic coordination polymers have attracted intense attention owing to their unique structure and morphology, tailorable compositions, as well as numerous applications.[5] The integration of the advantages of coordination polymers with spherical structure would endow them more unique features and extend their applications.[6]

Plant polyphenols (for example, tannic acid, TA) contain large amount of catechol or galloyl groups, which have strong chelating ability with various metal ions. The metal–TA coordination polymers, as a subclass of metal–organic coordination polymers, have recently been investigated as a versatile platform for the functional surface engineering.[7] As the polyphenols are known to strongly bind to various substrates throng covalent and non-covalent,[8] the controlling over the morphology and structure of such metal–phenolic coordination polymers usually relies on the shape of the external substrate (or template).[7a] Dopamine molecule contains one catechol group, which can chelate with metal ions. Metal-loaded polydopamine spheres with tunable compositions have been well-studied.[3c,9] However, there is very few examples for the synthesis of metal–plant polyphenol coordination spheres. Each TA ($C_{76}H_{52}O_{46}$) molecule contains five catechol groups and five galloyl groups to chelate with metal ions (Figure 1 a). The self-assembly between TA and metal ions is more complicated than that of dopamine. To date, most of the metal–phenolic coordination spheres were synthesized using the inorganic (or organic) sphere as a sacrificial template, resulting into a hollow structure. Ejima et al. successfully synthesized metal–TA coordination polymer capsules by a layer-by-layer assembly strategy using polystyrene spheres as a sacrificial template.[7a] Owing to the complicated polymerization process of the TA molecule and strong coordination interactions between TA and metal ions, the synthesis of metal–TA coordination spheres without using any spherical template is still a huge challenge.[10]

Herein, inspired from Stöber method for the synthesis of colloidal spheres, we report a formaldehyde-assisted metal–ligand crosslinking strategy for the synthesis of metal–phenolic coordination spheres with uniform diameter (ca. 300 nm) and tunable compositions. The formation of spherical metal–phenolic coordination polymer involves the pre-crosslinking of TA by formaldehyde in the alkaline ethanol/water solvents, followed by the aggregation assembly of polyphenol oligomers via metal–ligand crosslinking. Owing to the diverse chelation ability of TA, a range of mono-metal (such as Co^{2+}, Fe^{2+}, Fe^{3+}, Al^{3+}, Ni^{2+}, Cu^{2+}, Zn^{2+}, and Ce^{3+}), bi-metal (such as Fe-Co, Co-Zn), and multi-metal (such as Fe-Co-Ni-Cu-Zn) species can be successfully incorporated into the frameworks of the coordination spheres. Owing to the unique spherical structure and the metal–phenolic network, these coordination spheres can be applied for reliable analysis of nucleic acid variants with single-nucleotide discrimination. Furthermore, such coordination sphere derived nanoporous

[*] Prof. J. Wei,[+] Dr. G. Wang,[+] Dr. F. Chen,[+] M. Bai, Prof. Y. Zhao
School of Life Science and Technology, The Key Laboratory of Biomedical Information Engineering of Ministry of Education
Xi'an Jiaotong University
Xi'an, Shaanxi 710049 (P. R. China)
E-mail: yxzhao@mail.xjtu.edu.cn
Dr. Y. Liang, Prof. H. Wang
Department of Chemical Engineering, Monash University
Clayton, Victoria 3800 (Australia)
Prof. D. Zhao
Department of Chemistry, State Key Laboratory of Molecular Engineering of Polymers, Shanghai Key Lab of Molecular Catalysis and Innovative Materials,iChEM, Fudan University
Shanghai 200433 (P. R. China)
[+] These authors contributed equally to this work.
Supporting information and the ORCID identification number(s) for the author(s) of this article can be found under: https://doi.org/10.1002/anie.201805781.

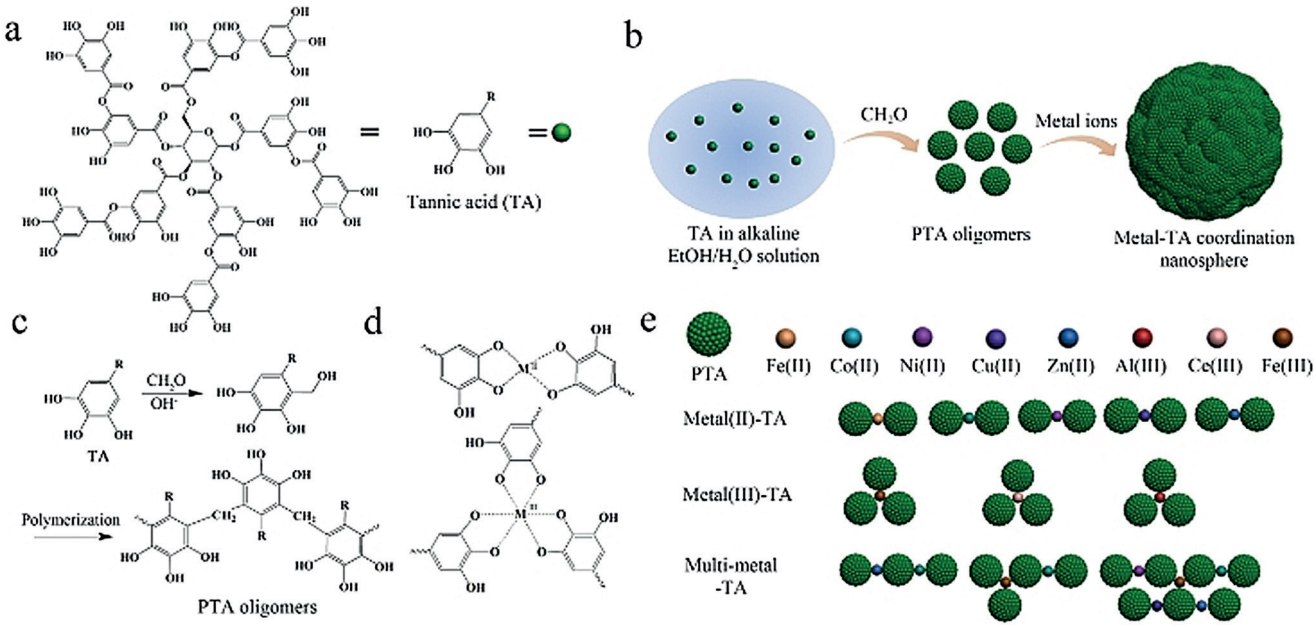

Figure 1. a) Chemical structure of TA. b) The synthesis of metal–phenolic coordination spheres. Step 1: polymerization of TA by formaldehyde to form poly(tannic acid) oligomers; Step 2: assembly of the oligomers to metal–TA coordination spheres via metal–ligand crosslinking. c) The possible formation of PTA oligomers via formaldehyde crosslinking. d) The formation of a metal–phenolic bond. e) The assembly units of metal–TA with various metal ions.

M/N-C (M = Fe, Co) composites exhibit high onset potential, large limiting current density, and good stability for the oxygen reduction reaction (ORR).

The synthesis of metal–phenolic coordination spheres mainly includes two steps (Figure 1 b). The first step is similar to the extended Stöber method for the synthesis of resorcinol–formaldehyde resin spheres.[3d] TA molecules were crosslinked by formaldehyde in the alkaline ethanol/water solvents (Figure 1 c; Supporting Information, Figure S1). As Pluronic F127 (polyethylene oxide-*block*-polypropylene oxide-*block*-polyethylene oxide) can interact with TA via hydrogen bonding, TA molecules may be trapped in the matrix of F127 block copolymers. As a result, TA molecules can be polymerized moderately by formaldehyde to form poly(tannic acid) (PTA) oligomers with the assistance of F127. In the second step, the polymer oligomers were further aggregated together to form metal–TA coordination spheres owing to the strong metal–ligand coordination interactions between the metal ions (such as Co^{2+}) and catechol groups from polymer oligomers (Figure 1 d). As the catechol groups have strong chelate ability with various metal ions, mono-metal (Co^{2+}, Fe^{2+}, Fe^{3+}, Al^{3+}, Ni^{2+}, Cu^{2+}, Zn^{2+}, and Ce^{3+}), bi-metal (such as Zn-Co and Fe-Co) and multi-metal species (Fe-Co-Ni-Cu-Zn) could be used as a crosslinker (Figure 1 e). To make the coordination spheres more stable, hydrothermal treatment was further applied to crosslink the organic ligands. Moreover, the TA polymer spheres without any metal species were also synthesized by direct hydrothermal treatment of PTA oligomers.

Scanning electron microscopy (SEM) image for PTA without using any metal crosslinker shows uniform spherical morphology, with diameter of around 300 nm (Figure 2 a). When metal ions are used as a crosslinker, the obtained polymers also exhibit spherical morphology (Figure 2 b,c; Supporting Information, Figure S2a–f), indicating the formation of metal-phenolic coordination spheres. In this work, eight kinds of metal ions such as Co^{2+}, Fe^{2+}, Fe^{3+}, Al^{3+}, Ni^{2+}, Cu^{2+}, Zn^{2+}, and Ce^{3+} are used as a crosslinker. All the

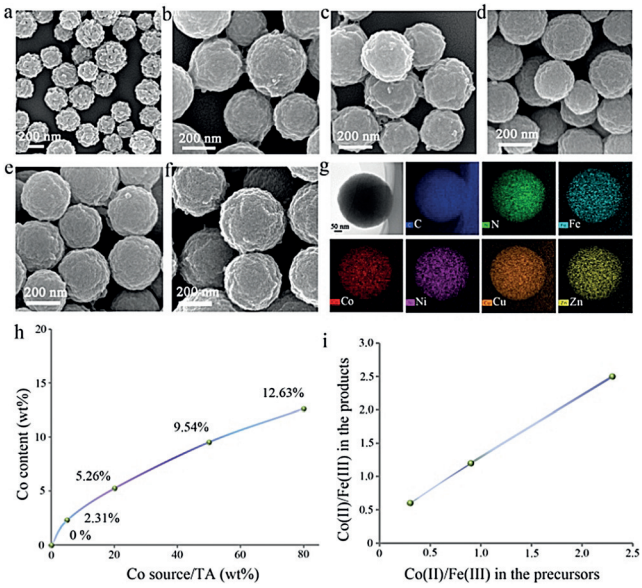

Figure 2. SEM images of a) PTA spheres, b) Co^{II}-TA, c) Fe^{III}-TA, d) Co^{II}-Zn^{II}-TA, e) Co^{II}-Fe^{III}-TA, and f) Fe^{III}-Co^{II}-Ni^{II}-Cu^{II}-Zn^{II}-TA coordination polymer spheres. g) TEM and corresponding element mapping images for Fe^{III}-Co^{II}-Ni^{II}-Cu^{II}-Zn^{II}-TA coordination polymer spheres. h) The cobalt contents in the Co-TA spheres when the mass ratio of cobalt source to TA increases. i) The molar ratio of Co^{II} to Fe^{III} in the Co^{II}-Fe^{III} coordination spheres when the molar ratio of Co^{II} to Fe^{III} in the precursors increases.

obtained metal–phenolic coordination polymers show spherical morphology. To further validate the universality of this strategy, mixed metal precursors such as $Co(NO_3)_2/Fe(NO_3)_3$, $Co(NO_3)_2/Zn(NO_3)_2$, $Co(NO_3)_2/FeSO_4$, and $Fe(NO_3)_3/Co(NO_3)_2/Ni(NO_3)_2/Cu(NO_3)_2/Zn(NO_3)_2$ were used as a metal source for crosslinking. Consequently, bimetal-TA (Co^{II}-Fe^{III}-TA, Co^{II}-Zn^{II}-TA and Co^{II}-Fe^{II}-TA), and multi-metal-TA (Fe^{III}-Co^{II}-Ni^{II}-Cu^{II}-Zn^{II}-TA) coordination spheres were obtained, respectively. All of these metal–phenolic coordination polymers reveal the spherical morphology and uniform diameter (Figure 2 d,e,f; Supporting Information, Figure S2g). The element mapping results for Co^{II}-Fe^{III}-TA reveal that Co and Fe species are distributed uniformly in the coordination spheres (Supporting Information, Figure S3). Even for the Fe^{III}-Co^{II}-Ni^{II}-Cu^{II}-Zn^{II}-TA coordination polymer sphere, it can be clearly seen that Fe, Co, Ni, Cu, and Zn elements are dispersed in the polymer spheres uniformly (Figure 2 g).

The metal contents for the metal–phenolic coordination polymers can also be easily adjusted by changing the amount of metal source. When the mass ratio of cobalt source (that is, $Co(NO_3)_2{\cdot}6H_2O$) to TA increased from 5 to 80 wt %, all the obtained Co-TA coordination polymers show spherical morphology (Supporting Information, Figure S4a–d). The content of cobalt in the coordination polymers increases from 2.3 to 12.6 wt %, calculated from thermogravimetric analysis (Figure 2 h; Supporting Information, Figure S4e). Moreover, the compositions of bimetal–TA coordination sphere can also be simply adjusted by changing the ratio of metal sources. For example, when the molar ratio of Co^{II} to Fe^{III} precursor is 0.8:1, 1.4:1, and 2.8:1 respectively, the obtained Co^{II}-Fe^{III}-TA coordination polymers show spherical morphology (Supporting Information, Figure S5). Energy-dispersive X-ray analysis (EDX) results reveal the molar ratio of Co^{II} to Fe^{III} is 0.6:1, 1.2:1, and 2.5:1 respectively (Figure 2 i).

The X-ray diffraction (XRD) results show that the metal–phenolic coordination spheres show amorphous structure (Supporting Information, Figure S4f). N_2 sorption isotherms reveal that these coordination spheres show very low surface area (10–20 $m^2 g^{-1}$), indicating nearly no nanopores in the polymer framework (Supporting Information, Figure S6, Table S1). X-ray photoelectron spectroscopy (XPS) of Co-TA coordination sphere further demonstrates the existence of cobalt species in the polymer (Supporting Information, Figure S7a). The high-resolution Co 2p spectrum reveals two peaks at 779.96 and 783.79 eV, which can be ascribed to the Co^{II}-O and Co^{II} salts, respectively (Supporting Information, Figure S7b).[11] The formation of Co^{II}–O bonds in the Co-TA coordination spheres can be further confirmed by the Raman spectra (Supporting Information, Figure S8).

To investigate the possible formation mechanism of the metal–phenolic coordination spheres, the samples at different stages were characterized by SEM. In the first step, the TA molecules were crosslinked by formaldehyde for 24 h. SEM results show the colloidal spheres are not formed yet at this stage (Figure 3 a). When the metal source (cobalt nitrate) was added into the TA–formaldehyde solution, the metal–TA coordination spheres were formed after stirring for 5 min (Figure 3 b). After further stirring for 24 h, the spherical

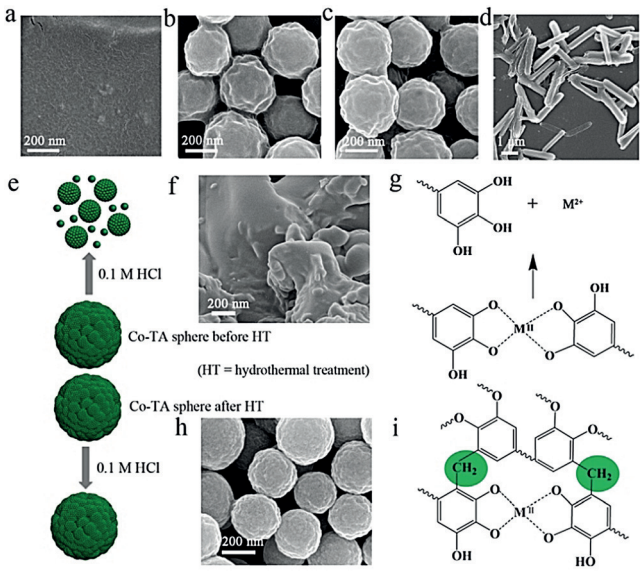

Figure 3. SEM images of a) PTA oligomers before addition of metal ions, Co-TA coordination spheres after addition of cobalt ions for b) 5 min, c) 24 h, and d) Co-TA coordination rods without using formaldehyde as a crosslinker. e) Represenation of the stability of the Co-TA coordination in the acid conditions. SEM images of f) Co-TA spheres without hydrothermal treatment (HT) in 0.1 M HCl, and h) Co-TA spheres after hydrothermal treatment at 100 °C in 0.1 M HCl. g) The reaction for the metal–TA coordination under acid conditions. i) The possible structure for the Co-TA sphere after HT.

structure was not changed obviously (Figure 3 c). After hydrothermal treatment at 100 °C for 24 h, the spherical morphology retains. The metal–TA coordination spheres before hydrothermal treatment can be quickly dissolved in 0.1 M HCl solution. This indicates the polymer spheres were formed by metal–ligand crosslinking (Figure 3 e,f,g). Comparably, the metal–TA coordination spheres after hydrothermal treatment is stable in 0.1 M HCl at least for 12 h (Figure 3 h). These results show that the organic ligands in the coordination spheres can be further polymerized during hydrothermal treatment, which can stabilize the spherical morphology and dramatically improve the acidic tolerance of the coordination spheres (Figure 3 i). When the formaldehyde was absent in the synthesis, only metal–TA rods were obtained (Figure 3 d), indicating an important role of formaldehyde in the formation of coordination sphere.

Based on the above results, we speculate the formation mechanism of metal–phenolic coordination spheres mainly includes two steps. In the first step, TA molecules were pre-crosslinked by formaldehyde. Like other phenols (such as resorcinol), formaldehyde can induce the polymerization of TA, resulting in the formation of TA–formaldehyde resin. In the weak alkaline ethanol/water solution, this polymerization reaction can be well controlled. As a result, low-molecular-weight PTA oligomers were obtained. In the second step, the PTA oligomers were further aggregated together to form metal–phenolic spheres by the metal–ligand crosslinking. Different from the conventional phenols (such as resorcinol), TA has abundant of catechol groups. After crosslinking by formaldehyde, PTA oligomers would still have enough

catechol groups to chelate with metal ions to form coordination polymers. When formaldehyde was not used to crosslink the TA, metal–TA coordination rods can be synthesized. This may be due to the fast polymerization rate of metal ions and TA. Comparing with the formation of polymer rods, the formaldehyde crosslinking of polyphenol may weaken the interactions between polyphenol and metal ions by decreasing the numbers of catechol groups. As a result, the metal–ligand assembly can proceed in a mild manner, and the thermodynamic stable spheres are obtained.

Fluorescent nanoprobes have shown promising applications for detection of biomolecules. As a proof-of-concept application, the metal–phenolic coordination spheres were used as effective fluorescence sensing platform for the analysis of nucleic acid variants such as miRNA (Supporting Information, Figure S9). The fluorophore-labeled single-stranded DNA probe is adsorbed and quenched by the metal–phenolic coordination polymer spheres, whereas fluorescence recovery is observed as the addition of complementary target miR-21 even down to 2 nM (Figure 4a). This

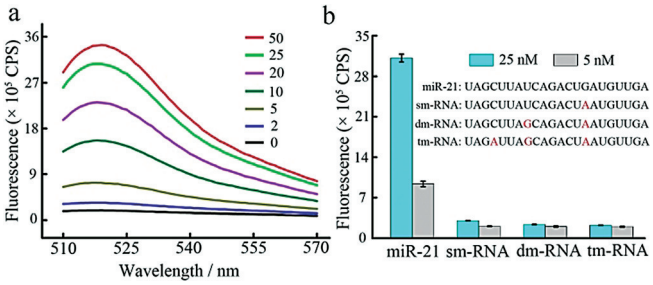

Figure 4. a) Fluorescent recovery in different concentrations [nM] of miR-21 solution. b) Selectivity for the detection of miR-21.

indicates a high affinity of single-stranded nucleic acids rather than double-stranded ones on these spheres. It is well-known that double-stranded nucleic acids seal phosphates and nitrogenous bases in the double helix structure. Therefore, we reason that such high affinity is mainly ascribed to the coordination interactions (between metal ions and nitrogenous bases/backbone phosphates) and π–π stacking interactions (between phenolic rings and nitrogenous base rings). These synergetic interactions could significantly improve the assay performance. The nanomolar sensitivity is consistent with those of traditional DNA probes such as molecular beacons. Moreover, such nanoprobe system can even distinguish miRNA homogeneous sequences with single nucleotide variation (Figure 4b). This sequence specificity is superior to those of other MOF nanoprobes and traditional DNA probes (Supporting Information, Table S2).

The conversion of biomass into valuable carbon composites as an efficient non-precious metal catalyst for ORR is desirable and challenging for the development of commercially viable fuel-cell technologies. Owing to the low cost and nontoxicity of the plant polyphenol and tunable compositions of metal–phenolic coordination polymers, the metal–phenolic coordination spheres were used as a sustainable carbon source to fabricate M/N-C (M = Fe, Co) based catalysts for ORR. Co-TA, Fe-TA and Co^{II}-Fe^{III}-TA coordination spheres were used as a precursor. Dicyandiamide was used as a N source. After gridding with coordination polymers and N source in the mortar, the composites were carbonized at 800 °C in N_2 atmosphere for 3 h. After the acid etching to remove the exposed metal (or metal carbide) nanoparticles, the carbon catalysts were obtained, which were denoted Co-TA-C800, Fe-TA-C800, and Co-Fe-TA-C800, respectively. TEM and XRD results reveal the successful synthesis of the metal/N-doped carbon composites (Supporting Information, Figures S10, S11). The Co (or Fe_3C) nanoparticles are encapsulated by a few layers of graphitic carbon. Element mapping results show that the nitrogen element is doped in the carbon framework uniformly. N_2 sorption results show that the BET surface area of Co-TA-C800, Fe-TA-C800, and Co-Fe-TA-C800 is 477, 328, 449 $m^2 g^{-1}$ respectively (Supporting Information, Figure S12, Table S1). XPS results reveal the existence of nitrogen species in the carbon framework (Supporting Information, Figure S13). High-resolution N 1s spectra prove the existence pyridinic and graphitic N with relative content of 34.3 and 60.1 at %, which is beneficial to improving the catalytic performance.[12]

The ORR performance of metal–phenolic coordination polymer-derived catalysts was evaluated using a rotating disk electrode technique. Cyclic voltammetry (CV) curves reveal a clear oxygen reduction peak for all the materials, implying an oxygen reduction activity (Figure 5a; Supporting Information, Figure S14). The linear scan voltammogram (LSV) curves for commercial Pt/C, Co-TA-C800, Fe-TA-C800, and Co-Fe-TA-C800 at the rotating speed of 1600 rpm in O_2-saturated 0.1 M KOH solution show their onset potentials are at 0.95, 0.93, 0.95, and 0.96 V (vs. reversible hydrogen electrode, RHE), respectively (Figure 5b). The onset potential for Co-Fe-TA-C800 is slightly higher than that of Pt/C,

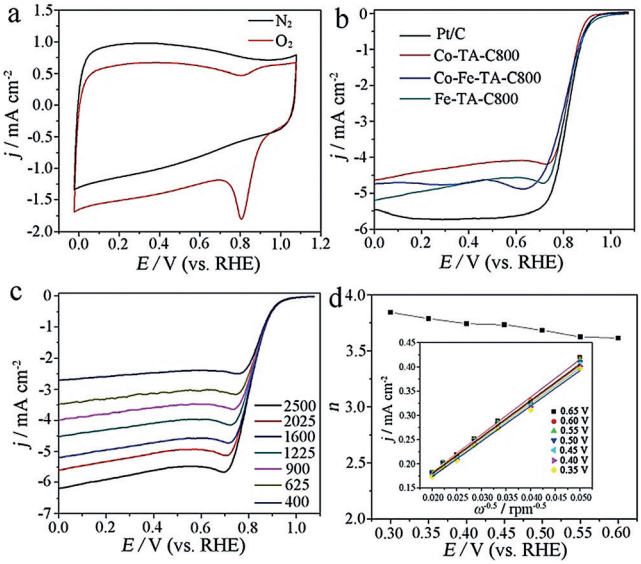

Figure 5. a) CV curves for Co-Fe-TA-C800. b) LSV curves for Pt/C, Co-TA-C800, Fe-TA-C800 and Co-Fe-TA-C800 in O_2-saturated 0.1 M KOH electrolyte at a rotating speed of 1600 rpm. c) LSV curves for Co-Fe-TA-C800 at different rotating speeds. d) Electron transfer numbers and K-L plots (inset) for Co-Fe-TA-C800.

Co-TA-C800 and Fe-TA-C800, indicating a high catalytic activity. The corresponding limiting current density at 0.30 V is 5.7, 4.3, 4.8, and 4.8 mA cm^{-2} for Pt/C, Co-TA-C800, Fe-TA-C800, and Co-Fe-TA-C800, respectively. The Koutechy–Levich plots of Co-TA-C800, Fe-TA-C800, and Co-Fe-TA-C800 exhibit good linearity with a similar slope (Figure 5 c,d; Supporting Information, Figures S15, S16), indicating a first-order reaction and similar electron transfer numbers (n). The n value at potential of 0.3 V for Co-TA-C800, Fe-TA-C800, and Co-Fe-TA-C800 is 3.91, 3.88, and 3.84 respectively, implying a near four-electron pathway. The catalytic performance is among the best of non-precious metal catalysts reported to date (Supporting Information, Table S3). The high catalytic performance may be ascribed to the synergetic catalytic effect between graphitic carbon layers activated by the encapsulated Fe_3C (or Co) nanoparticles and Fe (or Co)/N-C species in the catalysts.[10] Moreover, the catalysts derived from metal–phenolic coordination spheres show higher catalytic activity than other metal–phenolic catalysts (Supporting Information, Figure S17). Because of the enhanced surface area, more numbers of active sites would be exposed. The mass transport would also be enhanced owing to the nanoporous framework. Such catalysts also reveal better long-term stability than Pt/C (Supporting Information, Figure S18). Co-Fe-TA-C800 exhibits higher resistance to the methanol cross-over effect than Pt/C. These results demonstrate that metal–phenolic coordination polymer spheres are an excellent precursor to fabricate efficient electrode materials.

In summary, a formaldehyde-assisted metal–ligand cross-linking strategy is developed to synthesize metal–phenolic coordination spheres with unique morphology and tailorable compositions. TA molecules were firstly pre-crosslinked by formaldehyde to form PTA oligomers. Then, metal ions were used as a crosslinker to further assemble the PTA oligomers to metal–phenolic coordination spheres. These metal–phenolic coordination spheres can be applied as sensing platforms for the sensitive analysis of nucleic acid variants with single-nucleotide discrimination. It is further demonstrated that such colloidal metal–phenolic coordination spheres can be used as a precursor to fabricate functional carbon composites. The efficient catalytic activity for oxygen reduction reaction demonstrated that such metal–phenolic coordination spheres were an excellent precursor for the fabrication of carbon based electrode materials. It is believed that the formaldehyde-assistant metal–ligand crosslinking strategy would open up new avenues for the synthesis of advanced colloidal spheres with promising applications for biomedicine and electrochemical devices.

Acknowledgements

This work was financially supported by the National Science Foundation of China (No. 21475102, No. 31671013, No. 21701130, and No. 21705124), the China Postdoctoral Science Foundation (No. 2017M613102), the Fundamental Research Funds for the Central Universities and "Young Talent Support Plan" of Xi'an Jiaotong University.

Conflict of interest

The authors declare no conflict of interest.

Keywords: colloidal spheres · coordination polymers · electrocatalysis · plant polyphenol · sol–gel chemistry

How to cite: *Angew. Chem. Int. Ed.* **2018**, *57*, 9838–9843
Angew. Chem. **2018**, *130*, 9986–9991

[1] a) M. Oh, C. A. Mirkin, *Nature* **2005**, *438*, 651–654; b) X. M. Sun, Y. D. Li, *Angew. Chem. Int. Ed.* **2004**, *43*, 597–601; *Angew. Chem.* **2004**, *116*, 607–611; c) Y. N. Xia, B. Gates, Y. D. Yin, Y. Lu, *Adv. Mater.* **2000**, *12*, 693–713; d) F. Caruso, R. A. Caruso, H. Mohwald, *Science* **1998**, *282*, 1111–1114; e) E. Matijevic, *Acc. Chem. Res.* **1981**, *14*, 22–29; f) J. Liu, N. P. Wickramaratne, S. Z. Qiao, M. Jaroniec, *Nat. Mater.* **2015**, *14*, 763–774.

[2] W. Stöber, A. Fink, E. Bohn, *J. Colloid Interface Sci.* **1968**, *26*, 62–69.

[3] a) J. Liu, T. Yang, D. W. Wang, G. Q. Lu, D. Zhao, S. Z. Qiao, *Nat. Commun.* **2013**, *4*, 2798; b) W. Li, D. Zhao, *Adv. Mater.* **2013**, *25*, 142–149; c) K. Ai, Y. Liu, C. Ruan, L. Lu, G. Lu, *Adv. Mater.* **2013**, *25*, 998–1003; d) J. Liu, S. Z. Qiao, H. Liu, J. Chen, A. Orpe, D. Zhao, G. Q. Lu, *Angew. Chem. Int. Ed.* **2011**, *50*, 5947–5951; *Angew. Chem.* **2011**, *123*, 6069–6073.

[4] K. Sumida, K. Liang, J. Reboul, I. A. Ibarra, S. Furukawa, P. Falcaro, *Chem. Mater.* **2017**, *29*, 2626–2645.

[5] a) H. Li, M. Eddaoudi, M. O'Keeffe, O. M. Yaghi, *Nature* **1999**, *402*, 276–279; b) S. Kitagawa, R. Kitaura, S. Noro, *Angew. Chem. Int. Ed.* **2004**, *43*, 2334–2375; *Angew. Chem.* **2004**, *116*, 2388–2430; c) H. Furukawa, K. E. Cordova, M. O'Keeffe, O. M. Yaghi, *Science* **2013**, *341*, 974; d) J. Liu, L. Chen, H. Cui, J. Zhang, L. Zhang, C. Y. Su, *Chem. Soc. Rev.* **2014**, *43*, 6011–6061; e) S. Qiu, M. Xue, G. Zhu, *Chem. Soc. Rev.* **2014**, *43*, 6116–6140; f) V. Stavila, A. A. Talin, M. D. Allendorf, *Chem. Soc. Rev.* **2014**, *43*, 5994–6010; g) T. Zhang, W. Lin, *Chem. Soc. Rev.* **2014**, *43*, 5982–5993; h) Q.-L. Zhu, Q. Xu, *Chem. Soc. Rev.* **2014**, *43*, 5468–5512; i) A. H. Chughtai, N. Ahmad, H. A. Younus, A. Laypkov, F. Verpoort, *Chem. Soc. Rev.* **2015**, *44*, 6804–6849; j) T. Rodenas, I. Luz, G. Prieto, B. Seoane, H. Miro, A. Corma, F. Kapteijn, F. X. Llabres i Xamena, J. Gascon, *Nat. Mater.* **2015**, *14*, 48–55; k) T. R. Cook, Y. R. Zheng, P. J. Stang, *Chem. Rev.* **2013**, *113*, 734–777.

[6] a) X. P. Sun, S. J. Dong, E. K. Wang, *J. Am. Chem. Soc.* **2005**, *127*, 13102–13103; b) Y. M. Jeon, J. Heo, C. A. Mirkin, *J. Am. Chem. Soc.* **2007**, *129*, 7480–7481; c) I. Imaz, D. Maspoch, C. Rodriguez-Blanco, J. M. Perez-Falcon, J. Campo, D. Ruiz-Molina, *Angew. Chem. Int. Ed.* **2008**, *47*, 1857–1860; *Angew. Chem.* **2008**, *120*, 1883–1886; d) Y. M. Jeon, G. S. Armatas, J. Heo, M. G. Kanatzidis, C. A. Mirkin, *Adv. Mater.* **2008**, *20*, 2105–2110; e) N. R. Champness, *Angew. Chem. Int. Ed.* **2009**, *48*, 2274–2275; *Angew. Chem.* **2009**, *121*, 2309–2310; f) H. J. Lee, J. We, J. O. Kim, D. Kim, W. Cha, E. Lee, J. Sohn, M. Oh, *Angew. Chem. Int. Ed.* **2015**, *54*, 10564–10568; *Angew. Chem.* **2015**, *127*, 10710–10714; g) A. M. Spokoyny, D. Kim, A. Sumrein, C. A. Mirkin, *Chem. Soc. Rev.* **2009**, *38*, 1218–1227.

[7] a) H. Ejima, J. J. Richardson, K. Liang, J. P. Best, M. P. van Koeverden, G. K. Such, J. Cui, F. Caruso, *Science* **2013**, *341*, 154–157; b) J. Guo, Y. Ping, H. Ejima, K. Alt, M. Meissner, J. J. Richardson, Y. Yan, K. Peter, D. von Elverfeldt, C. E. Hagemeyer, F. Caruso, *Angew. Chem. Int. Ed.* **2014**, *53*, 5546–5551; *Angew. Chem.* **2014**, *126*, 5652–5657; c) K. Kim, M. Shin, M. Y. Koh, J. H. Ryu, M. S. Lee, S. Hong, H. Lee, *Adv. Funct. Mater.* **2015**, *25*, 2402–2410; d) P. Zhang, H. Li, G. M. Veith, S. Dai, *Adv. Mater.* **2015**, *27*, 234–239; e) J. Guo, B. L. Tardy, A. J. Christofferson, Y. Dai, J. J. Richardson, W. Zhu, M. Hu, Y. Ju, J.

Cui, R. R. Dagastine, I. Yarovsky, F. Caruso, *Nat. Nanotechnol.* **2016**, *11*, 1105 – 1111; f) H. Ejima, J. J. Richardson, F. Caruso, *Nano Today* **2017**, *12*, 136 – 148; g) P. Zhang, L. Wang, S. Yang, J. A. Schott, X. Liu, S. M. Mahurin, C. Huang, Y. Zhang, P. F. Fulvio, M. F. Chisholm, S. Dai, *Nat. Commun.* **2017**, *8*, 15020.

[8] Q. Wei, R. Haag, *Mater. Horiz.* **2015**, *2*, 567 – 577.

[9] a) Z. Wang, Y. Xie, Y. Li, Y. Huang, L. R. Parent, T. Ditri, N. Zang, J. D. Rinehart, N. C. Gianneschi, *Chem. Mater.* **2017**, *29*, 8195 – 8201; b) M. Xiao, Y. Li, M. C. Allen, D. D. Deheyn, X. Yue, J. Zhao, N. C. Gianneschi, M. D. Shawkey, A. Dhinojwala, *ACS Nano* **2015**, *9*, 5454 – 5460; c) M. Xiao, Z. Hu, Z. Wang, Y. Li, A. D. Tormo, N. L. Thomas, B. Wang, N. C. Gianneschi, M. D. Shawkey, A. Dhinojwala, *Sci. Adv.* **2017**, *3*, e1701151.

[10] a) J. Wei, Y. Liang, Y. Hu, B. Kong, J. Zhang, Q. Gu, Y. Tong, X. Wang, S. P. Jiang, H. Wang, *Angew. Chem. Int. Ed.* **2016**, *55*, 12470 – 12474; *Angew. Chem.* **2016**, *128*, 12658 – 12662; b) J. Wei, Y. Liang, Y. Hu, B. Kong, G. P. Simon, J. Zhang, S. P. Jiang, H. Wang, *Angew. Chem. Int. Ed.* **2016**, *55*, 1355 – 1359; *Angew. Chem.* **2016**, *128*, 1377 – 1381.

[11] X. Wang, L. L. Lu, Z. L. Yu, X. W. Xu, Y. R. Zheng, S. H. Yu, *Angew. Chem. Int. Ed.* **2015**, *54*, 2397 – 2401; *Angew. Chem.* **2015**, *127*, 2427 – 2431.

[12] a) K. Gong, F. Du, Z. Xia, M. Durstock, L. Dai, *Science* **2009**, *323*, 760 – 764; b) D. Guo, R. Shibuya, C. Akiba, S. Saji, T. Kondo, J. Nakamura, *Science* **2016**, *351*, 361 – 365.

Manuscript received: May 18, 2018
Revised manuscript received: June 19, 2018
Accepted manuscript online: June 21, 2018
Version of record online: July 5, 2018

